IEEE Photonics Journal
An IEEE Photonics Society Publication

Open Access

Efficiency Enhancement in Organic Solar Cells With Extended Resonance Spectrum of Localized Surface Plasmon

Volume 5, Number 4, August 2013

Fang Liu
Di Qu
Qi Xu
Xujie Pan
Kaiyu Cui
Xue Feng
Wei Zhang
Yidong Huang

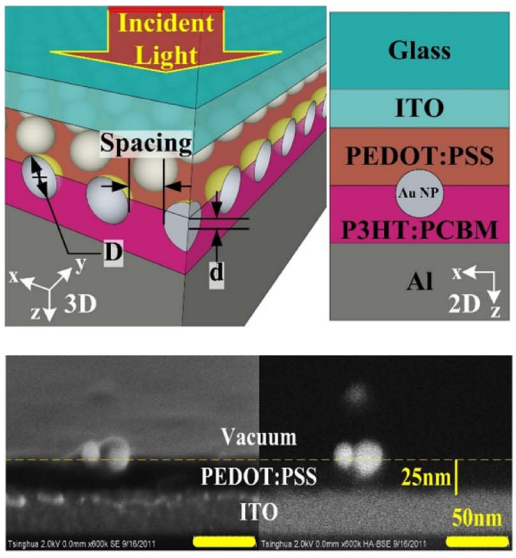

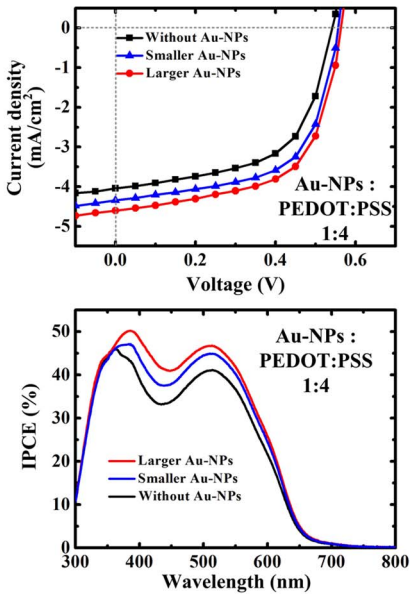

DOI: 10.1109/JPHOT.2013.2271715
1943-0655/$31.00 ©2013 IEEE

IEEE photonics SOCIETY

IEEE

Efficiency Enhancement in Organic Solar Cells With Extended Resonance Spectrum of Localized Surface Plasmon

Fang Liu, Di Qu, Qi Xu, Xujie Pan, Kaiyu Cui, Xue Feng, Wei Zhang, and Yidong Huang

Department of Electronic Engineering, Tsinghua National Laboratory for Information Science and Technology, Tsinghua University, Beijing 100084, China

DOI: 10.1109/JPHOT.2013.2271715

Manuscript received May 17, 2013; revised June 17, 2013; accepted June 18, 2013. Date of current version July 10, 2013. This work was supported in part by the National Basic Research Programs of China (973 Program) under Contracts 2013CBA01704, 2010CB327405, and 2011CBA00608, by the National High-Tech R&D Program (863 Program) under Contract 2011AA050504, and by the National Natural Science Foundation of China (NSFC) under Grants 61036011 and 61107050. Corresponding author: Y. Huang (e-mail: yidonghuang@tsinghua.edu.cn).

Abstract: The efficiency enhancement of thin film hetero-junction organic solar cells (OSCs) with Au-nanopaticles (Au-NPs) at the interface between the anode and active layers is studied theoretically and experimentally. It is demonstrated that the interface-Au-NPs could effectively extend the spectrum of light absorption enhancement based on the localized surface plasmon, which is revealed by the incident photon-to-current efficiency with photocurrent increased at both the long $(\lambda_0 = 600 \sim 700\ \text{nm})$ and short $(\lambda_0 = 400 \sim 500\ \text{nm})$ wavelength regions. The experiment results also indicate that the efficiency improvement of OSCs is related to the size and concentration of the Au-NPs. The optimized power conversion efficiency enhancement is about 25%.

Index Terms: (250.5403) Plasmonics, (040.5350) photovoltaic.

1. Introduction

Surface plasmon polariton (SPP) is transverse-magnetic surface electromagnetic excitation that propagates in a wavelike fashion along the interface between metal and dielectric medium [1], which could effectively enhance the light-matter interaction [2]–[4]. It was reported that the plasmonic metal nanoparticles (NPs) is promising for improving the efficiency of thin film solar cells [5]–[14]. This enhancement effect is much more significant for the solar cells with lower light absorption capacity [3], such as organic solar cells (OSCs) [5], [6], [10]–[12] and dye sensitized solar cells [13], [14].

The plasmonic metal NPs enhanced OSCs have attracted much attention. It is expected that the relative low efficiency could be greatly improved by trapping the light in the solar cells with metal NPs. For the hetero-junction OSCs with poly (3-exylthiophene): (6, 6)-phenyl-C61-butyric-acid-methyl ester (P3HT:PCBM) and poly (3, 4-ethylenedioxythiophene): poly (styrenesulfonate) (PEDOT:PSS) layers, metal NPs are introduced into the active layer (P3HT:PCBM) [10], [11] or the anode layer (PEDOT:PSS) [12], and the efficiency improvement was observed. However, the enhanced wavelength range is not wide enough, which limits the further increase of the efficiency of OSCs. Thus, by adopting different dielectric shells [15] or metal materials [11], [16], it is expected to adjust the localized surface plasmon (LSP) enhanced wavelength region and cover the solar spectrum with

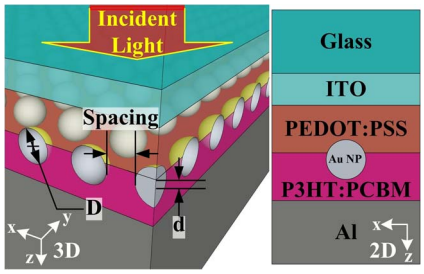

Fig. 1. Schematic diagram of the OSC with Au-NPs. The OSC consists of a glass substrate, a 20 nm-thick indium tin oxide (ITO) layer, a 30 nm-thick PEDOT:PSS anode layer, a 30 nm-thick P3HT:PCBM active layer, and a 100 nm-thick Al cathode layer. The periodic Au-NPs are located at the interface between PEDOT:PSS and P3HT:PCBM layers.

mixed NPs. Nevertheless, since metal NPs would affect the collection and transportation of photocurrent, the metal NPs introduced into the solar cells have the optimized concentration [10], [12], [13], which limited the number of metal NPs in OSCs. Therefore, to extend the resonance spectrum of a certain NPs is significant for getting higher efficiency enhancement of OSCs.

Recently, the mechanism of light absorption enhancement of OSCs with metal NPs has been studied theoretically, which indicated that the LSP mode dominates the light absorption enhancement of metal NPs [17]. It is anticipated that, by depositing the metal NPs at the interface between the active layer and the anode layer, the wavelength range of LSP enhancement could be extended for obtaining higher light absorption enhancement. In this paper, the hetero-junction OSCs with Au-NPs (referring as the "interface-Au-NPs") embedded at the interface between P3HT:PCBM and PEDOT:PSS layer are fabricated and measured. It is demonstrated that the incident photon-to-current efficiency (IPCE) is increased at not only long wavelength region $(\lambda_0 = 550 \sim 700$ nm$)$ but also short wavelength region $(\lambda_0 = 350 \sim 550$ nm$)$, and the power conversion efficiency (PCE) of OSCs is improved by about 25%. The experiment result proves that the LSP enhanced wavelength region could be effectively extended for obtaining stronger light absorption improvement.

2. Geometric Design and Simulation Results

Fig. 1(a) shows the schematic diagram of OSC with Au-NPs, which consists of the layers of glass substrate, indium tin oxide (ITO), PEDOT:PSS, periodic Au-NPs, P3HT:PCBM, and aluminum (Al) cathode. The Au-NPs are periodically distributed along *x* and *y* axis and located at the interface of PEDOT:PSS/ P3HT:PCBM layer. Although the Au-NPs are randomly distributed at the interface between the PEDOT:PSS and P3HT:PCBM layers in the fabricated OSCs rather than that shown in Fig. 1, the simulation result could well reveal the light absorption enhancement spectrum when comparing the simulation and experimental results shown below. A plane wave propagating along *z*-direction with unified amplitude is assumed as the input, and the optical properties including the wavelength dependent refractive index *n* and extinction coefficient *k* of the materials are taken from Refs. [18]–[21]. Based on the 3-D model of finite element method, the light absorption of OSCs with Au-NPs could be simulated and the detailed method can be seen in Ref. [17]. Different from Ref. [17], the Ag-NPs are replaced by the Au-NPs to be consistent with the experiment.

The simulation results shown in Fig. 2(a) illustrate the photon number spectra absorbed by the OSC without Au-NPs (black curve), with Au-NPs inside the P3HT:PCBM active layer (green curve), and with the "interface-Au-NPs" (blue curve). The photon number spectrum of the standard AM1. 5G [23] is also shown as the red curve. Comparing the blue and green curve with the black one, we can get the photon absorption enhancement of photo number as a function of wavelength, which is shown by Fig. 2(b). It is obvious that there are two absorption enhancement peaks for the OSCs with "interface-Au-NPs" shown as the blue line in Fig. 2(b), which results from the contact of the Au-NPs with two kinds of polymer materials and the excitation of LSP mode at both short and long wavelength region [17]. Although the peak of green curve in Fig. 2(b) is much higher than that of

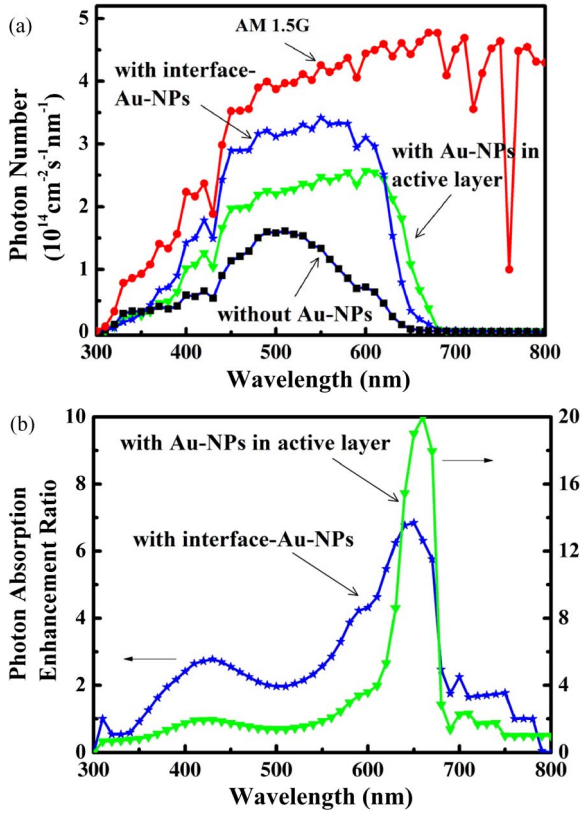

Fig. 2. (a) Absorption photon number spectra of OSC without Au-NPs (black square line), with Au-NPs totally embedded in P3HT:PCBM active layer (green triangle line), and with Au-NPs deposited at the interface between P3HT:PCBM active layer and PEDOT:PSS anode layer (blue star line), respectively. The red dotted line indicates the photon number spectrum of the standard AM1.5G. Here, the diameter *D* of Au-NPs is set as 28 nm. (b) Photon absorption enhancement of OSCs with interface-Au-NPs (blue curve) and Au-NPs in the active layer (green curve).

the blue one, the light absorption ability of OSCs is rather weak around wavelength of 650 nm and the absolute light absorption of green curve in Fig. 2(a) is less than that of the blue curve at short wavelength region. Therefore, the "interface-Au-NPs" could enhance the light absorption of OSCs more efficiently compared with the Au-NPs inside the active layer with just one peak shown as the green line in Fig. 2(b).

3. Fabrication Method and Measurement Results

Further, the thin film hetero-junction OSCs with and without Au-NPs are fabricated. The ITO-glass is adopted as the substrate and cleaned by the ethanol and deionized water. Then, a 25 nm-thick PEDOT:PSS (CLEVIOS P AI4083) layer and a 60 nm-thick P3HT:PCBM (with 1 : 1 weight ratio, SOLARMER) layer is spin-coated successively on the ITO-glass substrate. After depositing an Al layer as the cathode, the device is sealed with a UV-curing epoxy resin to finish the fabrication process of OSCs without Au-NPs. To realize the proposed interface-Au-NPs enhanced OSCs, the Au-NPs are prepared by sodium citrate reduction method [22] and blended into the PEDOT:PSS solution with different volume ratio (ratio of Au-NPs solution to PEDOT:PSS solution). Here, the size of Au-NPs could be altered easily by controlling the reaction time during synthesis. Instead of the simple PEDOT:PSS solution in the conventional fabrication process of OSCs, the PEDOT:PSS solution with Au-NPs is spin-coated onto the ITO-glass substrate. Fig. 3(a) and (b) shows the secondary electron image and backscattering electron image of scanning electron microscope (SEM) of the device after spin-coating the PEDOT:PSS solution with Au-NPs, which illustrates that

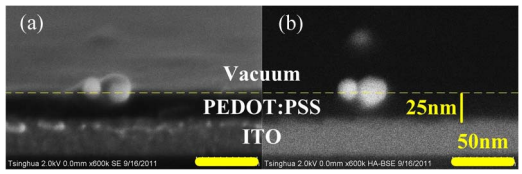

Fig. 3. SEM images of Au NPs located at the interface between PEDOT:PSS layer and vacuum. (a) Secondary electron images. (b) Backscattering electron image.

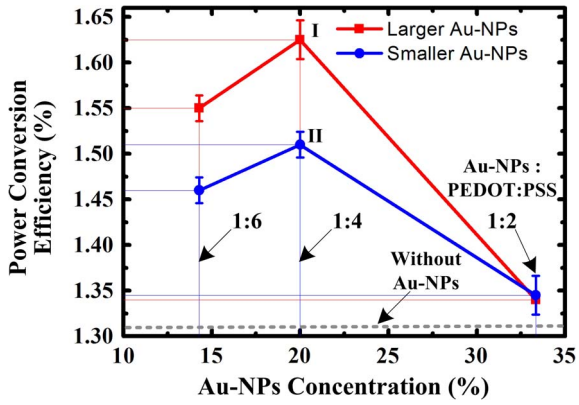

Fig. 4. Power conversion efficiency (PCE) as a function of Au-NPs concentration for larger (red curve, diameter in range of 20–40 nm) and smaller (blue curve, diameter in range of 10–25 nm) Au-NPs. The PCE value of the reference OSC without Au-NPs is 1.31% (the gray dashed line). For each OSC of different parameters, four devices are fabricated and measured.

part of the Au-NPs is inside the PEDOT:PSS layer and the other part is in air, which ensures that the Au-NPs could be located at the interface between PEDOT:PSS and P3HT:PCBM layers.

The OSCs with interface-Au-NPs having different size and concentration are fabricated, and four devices with the same parameters are prepared. The PCE indicating the ratio between the electric energy and the incident solar energy [24] is measured under the standard AM1.5G illumination at 100 mW/cm^{-2} (PECCELL PEC-L11). Fig. 4 shows the PCE of OSCs with larger (red curve, diameter in range of 20–40 nm) and smaller (blue curve, diameter in range of 10–25 nm) Au-NPs when varying the Au-NPs concentration. It is found that the OSCs with interface-Au-NPs have higher PCE values than the reference OSC (1.31%), which should result from the light absorption enhancement of LSP mode. The OSCs with larger interface-Au-NPs usually have better performance than those with smaller ones. The optimized volume ratio is 1 : 4 for both larger and smaller interface-Au-NPs and the highest efficiency enhancement is about 25% (PCE is increased from 1.31% to 1.625%) with larger Au-NPs.

Here, the optimized concentration of interface-Au-NPs improves the efficiency of OSCs and the lower efficiency improvement compared with the simulation prediction should be ascribed to the influence of the collection and transportation of photocurrent after introducing the interface-Au-NPs in the OSCs. It may also be noticed that the PCE is almost the same for OSCs with large and small metal nanoparticles. This can be understood for the following reason. Besides the LSP effect for enhancing the light trapping in thin film solar cells, the metal nanoparticles can also introduce the carrier combination. If the amount of nanoparticles exceed to the optimal value, more metal nanoparticles would lead to worse effect on the efficiency improvement of OSCs. This should be more serious for larger metal nanoparticles for the larger surface. Thus, the PCE could be rather close for large and small nanoparticles with concentration 33%.

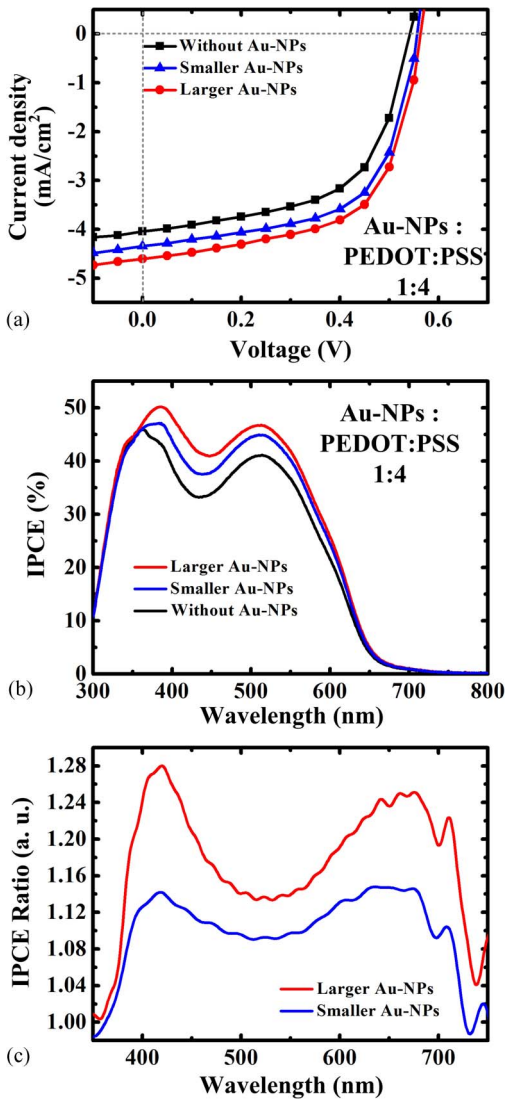

Fig. 5. (a) J-V characteristics of the OSCs with larger (red dot line) and smaller (blue triangle line) Au-NPs as well as that of the OSC without Au-NPs. (b) Corresponding IPCE curves as functions of wavelength. (c) IPCE ratios of larger Au-NPs (red line) and smaller Au-NPs (blue line) relative to the reference (without Au-NPs, black line).

To know more details of the efficiency improvement, the J-V characteristics and the corresponding IPCE are measured. Fig. 5(a) illustrates that, for OSCs with and without interface-Au-NPs, the open-circuit voltage is almost the same and the short-circuit current is increased significantly with the interface-Au-NPs, which means the efficiency increase results from the additional photocurrent generated in the OSCs and benefits from the light trapping of the Au-NPs with LSP effect. The IPCE demonstrating the ratio of the number of photons incident on a solar cell to the number of generated charge carriers [24] are obtained by using the PECCELL apparatus (PEC-S20). Fig. 5(b) illustrates the IPCE of the OSCs with larger Au-NPs (red curve), with smaller Au-NPs (blue curve), and without Au-NPs (black curve). Comparing the red and blue curve with the black one, the IPCE ratio can be derived and shown in Fig. 5(c), which depicts two obvious peaks around 420 nm and 650 nm. The previous theoretical result illustrated that, when metal NPs contact with two layers in OSCs with different dielectric constant, two corresponding LSP mode at different wavelength region could be excited and contribute to the light absorption enhancement [17].

Considering that the photocurrent is proportional to the absorbed light in the active layer, this measured results indicate that two resonance peaks of LSP mode is excited due to the contact of the Au-NPs with two different materials (P3HT:PCBM and PEDOT:PSS). Since the fabricated Au-NPs have non-uniform size and are randomly distributed at the interface of active layer, the measured enhancement ratio is of course different from the simulation one shown in Fig. 2(b). However, the obvious two enhancement peaks and their positions are consistent with the simulation results, which proves the above theoretical analysis.

Actually, the former reported results of OSCs with metal NPs could support our measurement results and corresponding explanation. The light absorption enhancement less than 500 nm had been observed when the Au-NPs are embedded inside the PEDOT:PSS layer,[1] and the obvious efficiency improvement in the wavelength region of 600–700 nm had been obtained with Au-NPs in the P3HT:PCBM layer.[2] Therefore, it is not strange that two resonance peaks of LSP are excited with the Au-NPs at the interface between two kinds of materials, which widen the absorption enhancement spectrum and consequently enhance the efficiency of OSCs. With the extension of LSP enhanced spectrum, the absolute efficiency of OSCs with "interface-Au-NPs", even though it is relatively low, could be rather high after optimizing the fabrication process of polymer layers of OSCs. And the proposed structure in this paper could be compatible with other novel techniques [25] for improving the efficiency of solar cells.

4. Conclusion

In conclusion, the plasmonic enhanced hetero-junction OSCs with extended resonance spectrum of LSP is studied theoretically and experimentally. Simulation result indicates that, by depositing the Au-NPs at the interface between the anode (PEDOT:PSS) and active (P3HT:PCBM) layer, the light absorption could be enhanced at both the long $(\lambda_0 = 600 \sim 700$ nm$)$ and short $(\lambda_0 = 400 \sim 500$ nm$)$ wavelength region due to the contact of the Au-NPs with two kinds of materials, which is validated by the experiment results by comparing the IPCE of proposed OSCs with that of one without Au-NPs. It is demonstrated that there exists the optimized concentration of Au-NPs for enhancing the efficiency of OSCs, which should be related to the collection and transportation of photocurrent. The efficiency of the OSCs is increased by 25%.

[1]The blue curve in [11, Fig. 2].

[2]In [9, Fig. 2(b)], the ratio of red curve to the black one demonstrates a peak surrounding $\lambda_0 = 620$ nm; in [10, Fig. 6], the ratio of red curve to the green one demonstrates a peak surrounding $\lambda_0 = 650$ nm.

References

[1] H. Raether, *Surface Plasmons*. Berlin, Germany: Springer-Verlag, 1988, pp. 4–13.
[2] G. Sun, J. B. Khurgin, and R. A. Soref, "Practical enhancement of photoluminescence by metal nanoparticles," *Appl. Phys. Lett.*, vol. 94, no. 10, pp. 101103-1–101103-3, Mar. 2009.
[3] J. B. Khurgin, G. Sun, and R. A. Soref, "Practical limits of absorption enhancement near metal nanoparticles," *Appl. Phys. Lett.*, vol. 94, no. 7, pp. 071103-1–071103-3, Feb. 2009.
[4] K. J. Russell, T. Liu, S. Cui, and E. L. Hu, "Large spontaneous emission enhancement in plasmonic nanocavities," *Nature Photon.*, vol. 6, no. 7, pp. 459–462, Jul. 2012.
[5] B. P. Rand, P. Peumans, and S. R. Forrest, "Long-range absorption enhancement in organic tandem thin-film solar cells containing silver nanoclusters," *J. Appl. Phys.*, vol. 96, no. 12, pp. 7519–7526, Dec. 2004.
[6] B. Niesen, B. P. Rand, P. V. Dorpe, H. Shen, B. Maes, J. Genoe, and P. Heremans, "Excitation of multiple dipole surface plasmon resonances in spherical silver nanoparticles," *Opt. Exp.*, vol. 18, no. 18, pp. 19032–19038, Aug. 2010.
[7] H. A. Atwater and A. Polman, "Plasmonics for improved photovoltaic devices," *Nature Mater.*, vol. 9, no. 3, pp. 205–213, Mar. 2010.
[8] D. Qu, F. Liu, J. F. Yu, W. L. Xie, Q. Xu, X. D. Li, and Y. D. Huang, "Plasmonic core-shell gold nanoparticle enhanced optical absorption in photovoltaic devices," *Appl. Phys. Lett.*, vol. 98, no. 11, pp. 113119-1–113119-3, Mar. 2011.
[9] X. Chen, B. Jia, J. K. Saha, B. Cai, N. Stokes, Q. Qiao, Y. Wang, Z. Shi, and M. Gu, "Broadband enhancement in thin-film amorphous silicon solar cells enabled by nucleated silver nanoparticles," *Nano Lett.*, vol. 12, no. 5, pp. 2187–2192, May 2012.
[10] D. H. Wang, D. Y. Kim, K. W. Choi, J. H. Seo, S. H. Im, J. H. Park, O. O. Park, and A. J. Heeger, "Enhancement of donor-acceptor polymer bulk heterojunction solar cell power conversion efficiencies by addition of Au nanoparticles," *Angew. Chem. Int. Ed.*, vol. 50, no. 4, pp. 5519–5523, Jun. 2011.

[11] G. D. Spyropoulos, M. Stylianakis, E. Stratakis, and E. Kymakis, "Plasmonic organic photovoltaics doped with metal nanoparticles," *Photon. Nanostruct.–Fundam. Appl.*, vol. 9, no. 2, pp. 184–189, Apr. 2011.
[12] F. C. Chen, J. L. Wu, C. L. Lee, Y. Hong, C. H. Kuo, and M. H. Huang, "Plasmonic-enhanced polymer photovoltaic devices incorporating solution-processable metal nanoparticles," *Appl. Phys. Lett.*, vol. 95, no. 1, pp. 013305-1–013305-3, Jul. 2009.
[13] Q. Xu, F. Liu, W. Meng, and Y. Huang, "Plasmonic core-shell metal-organic nanoparticles enhanced dye-sensitized solar cells," *Opt. Exp.*, vol. 20, no. S6, pp. A898–A907, Nov. 2012.
[14] M. D. Brown, T. Suteewong, R. S. S. Kumar, V. D. Innocenzo, A. Petrozza, M. M. Lee, U. Wiesner, and H. J. Snaith, "Plasmonic dye-sensitized solar cells using core-shell metal-insulator nanoparticles," *Nano Lett.*, vol. 11, no. 2, pp. 438–445, Feb. 2011.
[15] G. Xu, M. Tazawa, P. Jin, S. Nakao, and K. Yoshimura, "Wavelength tuning of surface plasmon resonance using dielectric layers on silver island films," *Appl. Phys. Lett.*, vol. 82, no. 22, pp. 3811–3813, Jun. 2003.
[16] H. Chen, S. Chou, W. Tseng, I. P. Chen, C. Liu, C. Liu, C. Liu, C. Chen, C. Wu, and P. Chou, "Large AuAg alloy nanoparticles synthesized in organic media using a one-pot reaction: Their applications for high-performance bulk heterojunction solar cells," *Adv. Funct. Mater.*, vol. 22, no. 19, pp. 3975–3984, Oct. 2012.
[17] D. Qu, F. Liu, X. J. Pan, W. L. Xie, Q. Xu, and Y. D. Huang, "Mechanism of optical absorption enhancement in thin film organic solar cells with plasmonic metal nanoparticles," *Opt. Exp.*, vol. 19, no. 24, pp. 24 795–24 803, Nov. 2011.
[18] H. Hoppe, N. S. Sariciftci, and D. Meissner, "Optical constants of conjugated polymer/fullerene based bulk heterojunction organic solar cells," *Mol. Cryst. Liquid Cryst.*, vol. 385, no. 1, pp. 113–119, Jan. 2002.
[19] F. Monestier, J. J. Simon, P. Torchio, L. Escoubas, F. Flory, S. Bailly, R. de Bettignies, S. Guillerez, and C. Defranoux, "Modeling the short-circuit current density of polymer solar cells based on P3HT:PCBM blend," *Solar Energy Mater. Solar Cells*, vol. 91, no. 5, pp. 405–410, Mar. 2007.
[20] A. D. Raki, "Algorithm for the determination of intrinsic optical constants of metal films: Application to aluminum," *Appl. Opt.*, vol. 34, no. 22, pp. 4755–4767, Aug. 1995.
[21] E. D. Palik, *Handbook of Optical Constants of Solids*. Orlando, FL, USA: Academic, 1985.
[22] R. H. Bube, *Fundamentals of Solar Cells: Photovoltaic Solar Energy Conversion*. Amsterdam, The Netherlands: Elsevier, 1983, pp. 26–31.
[23] B. V. Enustun and J. Turkevich, "Coagulation of colloidal gold," *J. Amer. Chem. Soc.*, vol. 85, no. 21, pp. 3317–3328, Nov. 1963.
[24] W. C. H. Choy, *Organic Solar Cells: Materials and Device Physics*. London, U.K.: Springer-Verlag, 2013, pp. 12–13.
[25] Y. Zhang, H. Geng, Z. Zhou, J. Wu, Z. Wang, Y. Zhang, Z. Li, L. Zhang, Z. Yang, and H. Hwang, "Development of inorganic solar cells by nanotechnology," *Nano-Micro Lett.*, vol. 4, no. 2, pp. 124–134, 2012.